Numerical Analysis of the Legendre-Transformed Poisson–Boltzmann Electrostatics

Zunding Huang * Bo Li †

November 25, 2022

Abstract

The Legendre-transformed Poisson–Boltzmann (LTPB) electrostatic energy functional of electric displacements is a convex functional with which the principle of energy minimization can be applied to determine the equilibrium electrostatics. Recently, such a new formulation of continuum electrostatics has been used in several theoretical studies of charged systems. This work presents a systematic numerical analysis of the LTPB electrostatics. Instead of solving the Euler–Lagrange equation of the functional, we use an optimization method to minimize the functional after a finite-difference discretization and numerical integration. Application of the LTPB formulation to continuum molecular modeling results a constrained variational problem with an interface, the dielectric boundary, separating an underlying system region into two subregions of different dielectric permittivities. We construct approximate, penalized energy functionals, and prove the convergence of the minimizers and minimum values of such functionals. Algorithms of numerical optimization of the penalized functional are designed and implemented, and numerical tests are given to show the convergence. Finally, we develop numerical methods for minimizing a total energy of dielectric boundary consisting of both surface and electrostatic energy, and compare the LTPB and the classical Poisson–Boltzmann formulations of electrostatics. We present extensive numerical tests for a model spherical system to show that for a wide range of numerical parameters the LTPB formulation has advantages in terms of numerical accuracy and computational efficiency.

Key words and phrases: Poisson–Boltzmann theory, Legendre transform, penalty method, numerical optimization, convergence.

1 Introduction

The classical Poisson–Boltzmann (PB) theory [1, 8, 28] is a continuum theory for electrostatics of an ionic solution. It has been widely applied to biological physics, colloid science, and chemical engineering. In the PB theory, the electrostatic potential $\phi : \Omega \to \mathbb{R}$ is determined by the nonlinear PB equation

$$\nabla \cdot \varepsilon \nabla \phi - B'(\phi) = -f \qquad \text{in } \Omega, \tag{1.1}$$

together with some boundary conditions. Here, $\Omega \subseteq \mathbb{R}^3$ is the region occupied by the ionic solution, $\varepsilon : \Omega \to (0, \infty)$ is the dielectric coefficient, $B : \mathbb{R} \to \mathbb{R}$ is a given function with $-B'(\phi)$ being the ionic charge density, and $f : \Omega \to \mathbb{R}$ is a given function describing a fixed charge density. A typical example of the function B is, after non-dimensionalization, $B(s) = \cosh(s) - 1$ for a two-species 1:1 ionic system

*Department of Mathematics, University of California, San Diego, 9500 Gilman Drive, Mail code: 0112, La Jolla, CA 92093-0112, USA. Email: zuhuang@ucsd.edu.

†Department of Mathematics and Ph.D. Program in Quantitative Biology, University of California, San Diego, 9500 Gilman Drive, Mail code: 0112, La Jolla, CA 92093-0112, USA. Email: bli@math.ucsd.edu.

(each ion carries a $+1$ elementary charge in one of the species while -1 in the other). Another example is $B(s) = s^2/2$ with which (1.1) becomes the linearized PB equation. In general, the PB equation (1.1) is the Euler–Lagrange equation of the classical PB electrostatic energy functional [1,4,8,11,12,14,25,27]

$$I[\phi] = \int_\Omega \Big[-\frac{\varepsilon}{2} |\nabla \phi|^2 + f\phi - B(\phi) \Big] \, dx. \tag{1.2}$$

This functional is concave and can be maximized to yield the equilibrium electrostatic potential and energy. We refer to [4, 6] for discussions on the formulation of the electrostatic energy that leads to the maximization instead of minimization of the functional for equilibrium electrostatics. (Strictly speaking, $I[\phi]$ is an approximation of the electrostatic free energy as the term $B(\phi)$ includes the ionic entropy [4,14]. Since we only consider an underlying system with a fixed temperature, we will use the word "energy" instead of "free energy" for simplicity.)

In recent years, a Legendre-transformed Poisson–Boltzmann (LTPB) electrostatic energy functional has been constructed and used in theoretical studies of charged systems [3,6,21–23]. This is a functional of electric displacements $D : \Omega \to \mathbb{R}^3$, given by

$$J[D] = \int_\Omega \left[\frac{1}{2\varepsilon} |D|^2 + B^*(f - \nabla \cdot D) \right] dx + \int_{\partial\Omega} gD \cdot n \, dS, \tag{1.3}$$

where B^* is the Legendre transform of the function B and $g : \partial\Omega \to \mathbb{R}$ is a given function that corresponds to the Dirichlet boundary condition $\phi = g$ on $\partial\Omega$ for the classical PB equation (1.1). We recall that the Legendre transform $h^* : \mathbb{R} \to \mathbb{R} \cup \{+\infty\}$ for a given function $h : \mathbb{R} \to \mathbb{R}$ is defined by $h^*(\xi) = \sup_{s \in \mathbb{R}} [s\xi - h(s)]$ for all $\xi \in \mathbb{R}$ [26, 34]. If h is smooth and strictly convex, and ξ is in the range of h', then $h^*(\xi) = s\xi - h(s)$ and $h^{*\prime}(\xi) = s$, where s is uniquely determined by $h'(s) = \xi$.

The key property of the new, LTPB functional (1.3) is that it is strictly convex. The minimization of the functional determines the equilibrium electric displacement and the minimum value of the energy, consistent with the general principle of energy minimization. Moreover, the LTPB functional (1.3) can be regarded as dual to the classical PB functional (1.2). The dual variable, the electric displacement D, and the primary variable, the electrostatic potential ϕ, are related by $D = -\varepsilon \nabla \phi$. In fact, Ciotti and Li [6] have obtained the duality of the LTPB and PB formulations: $I[\phi] \le J[D]$ for any admissible ϕ and D; and there exist a unique maximizer $\phi_{\rm m}$ of I and a unique minimizer $D_{\rm m}$ of J, related by $D_{\rm m} = -\varepsilon \nabla \phi_{\rm m}$, and $J[D_{\rm m}] = I[\phi_{\rm m}]$.

Ciotti and Li [6] also propose to apply the LTPB framework to the continuum modeling of solvation of charged molecules (e.g., proteins) in water, where the region Ω is separated by an interface Γ, called a dielectric boundary, into the molecular region Ω_-, interior of Γ, and the water region Ω_+, exterior of Γ [2, 4, 8, 9, 14, 28, 31, 32]. Specifically, they construct the LTPB electrostatic energy functional

$$J_\Gamma[D] = \int_\Omega \left[\frac{1}{2\varepsilon_\Gamma} |D|^2 + \chi_+ B^*(f - \nabla \cdot D) \right] dx + \int_{\partial\Omega} gD \cdot n \, dS, \tag{1.4}$$

Here, $\varepsilon_\Gamma : \Omega \to \mathbb{R}$ is the dielectric coefficient defined via the dielectric boundary Γ by $\varepsilon_\Gamma(x) = \varepsilon_-$ if $x \in \Omega_-$ and $\varepsilon_\Gamma(x) = \varepsilon_+$ if $x \in \Omega_+$, where ε_- and ε_+ are two distinct positive constants, and χ_+ is the characteristic function of Ω_+. It is proved in [6] that the minimization of this LTPB functional over all the electric displacements D constrained by $\nabla \cdot D = f$ in Ω_- is equivalent (in terms of duality) to the maximization of the classical PB electrostatic energy functional

$$I_\Gamma[\phi] = \int_\Omega \Big[-\frac{\varepsilon_\Gamma}{2} |\nabla \phi|^2 + f\phi - \chi_+ B(\phi) \Big] \, dx, \tag{1.5}$$

among all the electrostatic potentials ϕ satisfying the boundary condition $\phi = g$ on $\partial\Omega$.

In a variational approach to the continuum modeling of the solvation of charged molecules, one minimizes a total energy that includes the electrostatic and other energy terms [4, 9, 14, 31, 32]. In a simple setting, the total energy is

$$G[\Gamma] = \gamma_0 \text{Area}\,(\Gamma) + E_{\text{ele}}[\Gamma], \tag{1.6}$$

where $\gamma_0 > 0$ is the constant surface tension and $E_{\text{ele}}[\Gamma]$ is the electrostatic energy, given by

$$E_{\text{ele}}[\Gamma] = \max_{\phi = g \text{ on } \Omega} I_\Gamma[\phi] = \min_{\nabla \cdot D = f \text{ in } \Omega_-} J_\Gamma[D]. \tag{1.7}$$

Numerical minimization of the functional $G[\Gamma]$ can be done by a gradient descent iteration that updates the boundary Γ_k in the kth step. For the LTPB formulation, this is a min-min iteration: minimizing $J_{\Gamma_k}[D]$ over D and then minimizing $G[\Gamma]$ with Γ_k as an initial guess. The PB formulation leads to a max-min process: maximizing $I_{\Gamma_k}[\phi]$ over ϕ and then minimizing $G[\Gamma]$ with Γ_k as an initial guess. Whether the min-min algorithm is more stable and efficient than the max-min algorithm for large-scale computations poses a question of much practical interest.

In this work, we present a systematic numerical analysis of the LTPB electrostatics, particularly applied to the dielectric boundary problem. There are many different numerical schemes we can use to solve our underlying variational problems. Instead of testing different methods, we focus on the development of efficient approaches for the numerical minimization of the LTPB functional that may be applied to large-scale molecular simulations. We also compare the two LTPB and PB formulations in terms of numerical computations.

Our main results are the following:

(1) We develop and implement a numerical method to minimize the LTPB functional (1.3) without interface. This method consists of the discretization of the functional by a finite-difference scheme and the composite trapezoidal quadrature rule, and the optimization of the resulting function by a gradient descent method. We present numerical tests to show the convergence of our method.

(2) To minimize numerically the functional J_Γ defined in (1.4) among all the displacements D constrained by $\nabla \cdot D = f$ in Ω_-, we propose a penalty method: minimize the penalized functional

$$J_{\Gamma,\mu}[D] = \int_\Omega \left[\frac{1}{2\varepsilon_\Gamma} |D|^2 + \chi_+ B^*(f - \nabla \cdot D) + \frac{\chi_-}{2\mu} |\nabla \cdot D - f|^2 \right] dx, \tag{1.8}$$

without the constraint, where $\mu > 0$ is a penalty parameter and χ_- is the characteristic function of Ω_-. We prove that, as $\mu \to 0$, the minimizers and mimimum values of the penalized functionals $J_{\Gamma,\mu}$ converge to those for the functional J_Γ with the constraint. We then discretize the functional by a finite-difference scheme and a numerical quadrature, and implement a limited-memory Broyden–Fletcher–Goldfarb–Shanno (BFGS) method to minimize numerically the resulting convex function. We report numerical tests to validate the convergence of our method.

(3) We construct a max-min method and a min-min method to minimize numerically the total energy $G[\Gamma]$ (1.6), and implement these methods for a radially symmetric system. We present extensive numerical tests to examine the accuracy, efficiency, and stability of the LTPB and PB formulations of electrostatics, respectively.

We note that the explicit formula of the Legendre transform $B^* = B^*(\xi)$ of a given convex function $B = B(s)$ is generally not available. One can, however, generate a table of values $B^*(\xi)$ for selected values of $\xi \in [\xi_{\min}, \xi_{\max}]$, where the numbers $\xi_{\min}$ and $\xi_{\max}$ can be estimated from an underlying system. Note that, the convex function $B = B(s)$ used in the generalized PB theory for electrostatic interactions with ionic size effect is only implicitly defined [13, 16, 33]. One can solve a system of nonlinear algebraic equations to obtain the value of $B(s)$ for s in an interval of the real line and then calculate $B^*(\xi)$ to generate a table. We also note that, for a general dielectric boundary problem,

the level-set method can be used to define the boundary, and to minimize a total energy that has the electrostatic and other parts of the energy; cf. [32]. Along this line, it will be interesting to use the level-set method to minimize such a total energy of dielectric boundaries and compare the min-min and max-min algorithms, and hence compare the LTPB and PB formulations in terms of numerical computations.

The rest of this paper is organized as follows: In section 2, we present the finite-difference discretization, numerical integration, and the gradient descent method for minimizing the LTPB functional without interface, and the numerical results to show the convergence. In section 3, we study the LTPB functional for a system with a fixed dielectric boundary. We first present our penalized LTPB functionals and prove their convergence. We then construct and implement numerical discretization, integration, and optimization methods, and show such convergence by numerical tests. In section 4, we present our numerical methods for minimizing the total energy with both the surface and electrostatic energies. We test our methods for a radially symmetric system and present numerical results to compare the PB and LTPB formulations. In Appendix, we prove some analytic results for the model radially symmetric system.

2 Numerical Minimization of the LTPB Functional

2.1 A brief review of the theory

Let Ω be a bounded domain in $\mathbb{R}^3$ with a Lipschitz-continuous boundary $\partial\Omega$, $f \in L^2(\Omega)$, and $g \in H^1(\Omega)$. Let $\varepsilon \in L^\infty(\Omega)$ be such that $\varepsilon_{\min} \le \varepsilon(x) \le \varepsilon_{\max}$ for all $x \in \Omega$, where $\varepsilon_{\min}$ and $\varepsilon_{\max}$ are given positive constants. Let $B \in C^3(\mathbb{R})$ be a strictly convex function such that it is uniquely minimized at 0, $B(0) = 0$, and $B(\pm\infty) = \infty$. Note that the Legendre transform B^* of B is a strictly convex and C^2-function, minimized at 0 with the minimum value $B^*(0) = 0$. We consider the maximization of the classical PB electrostatic free-energy functional $I : H^1_g(\Omega) \to \mathbb{R} \cup \{-\infty\}$ defined in (1.2), where

$$H^1_g(\Omega) := \left\{ u \in H^1(\Omega) : u = g \text{ on } \partial\Omega \right\}. \tag{2.1}$$

The following theorem is proved in [15]:

Theorem 2.1 ([15]). *The functional $I : H^1_g(\Omega) \to \mathbb{R} \cup \{-\infty\}$ has a unique maximizer $\phi_{\rm m}$. Moreover, $\phi_{\rm m} \in L^\infty(\Omega)$, and it is the unique weak solution to the boundary-value problem of PB equation* (1.1).

We consider the minimization of the Legendre-transformed Poisson–Boltzmann (LTPB) functional $J : H(\mathrm{div}, \Omega) \to \mathbb{R} \cup \{+\infty\}$ with $J[D]$ defined in (1.3) and

$$H(\mathrm{div}, \Omega) := \left\{ D \in \left[L^2(\Omega)\right]^3 : \nabla \cdot D \in L^2(\Omega) \right\}. \tag{2.2}$$

We recall that $H(\mathrm{div}, \Omega)$ is a Hilbert space with the inner product

$$\langle D, G \rangle = \int_\Omega \left[D \cdot G + (\nabla \cdot D)(\nabla \cdot G) \right] dx \qquad \forall D, G \in H(\mathrm{div}, \Omega).$$

If $D \in H(\mathrm{div}, \Omega)$ and n is the unit exterior normal at the boundary $\partial\Omega$, then $D \cdot n \in L^2(\partial\Omega)$ [30].

The following theorem, proved in [6], provides the duality for the PB functional I defined in (1.2) and the LTPB functional J defined in (1.3):

Theorem 2.2 ([6]). *We have $I[\phi] \le J[D]$ for any $\phi \in H^1_g(\Omega)$ and any $D \in H(\mathrm{div}, \Omega)$, and $\sup_{\phi \in H^1_g(\Omega)} I[\phi] = \inf_{D \in H(\mathrm{div}, \Omega)} J[D]$. Moreover, if $\phi_{\rm m} = \arg\max_{\phi \in H^1_g(\Omega)} I[\phi]$, then $D_{\rm m} := -\varepsilon \nabla \phi_{\rm m} \in$*

$H(\mathrm{div},\Omega)$ *is the unique minimizer of* $J : H(\mathrm{div},\Omega) \to \mathbb{R} \cup \{+\infty\}$ *and the unique weak solution to the boundary-value problem of the Euler–Lagrange equation for the functional* $J : H(\mathrm{div},\Omega) \to \mathbb{R} \cup \{+\infty\}$

$$\begin{aligned} &\frac{D}{\varepsilon} + \nabla(B^{*\prime}(f - \nabla \cdot D)) = 0 \qquad \text{in } \Omega, \\ &B^{*\prime}(f - \nabla \cdot D) = g \qquad \text{on } \partial\Omega. \end{aligned}$$

2.2 Numerical methods and tests

We choose $\Omega = (0, L)^3$ for some $L > 0$, and fix $\varepsilon > 0$ to be a constant, $f \in L^2(\Omega)$, and $g \in H^1(\Omega)$. We fix the convex function B and calculate its Legendre transform B^*. Next, we cover $\overline{\Omega} = [0, L]^3$ with a uniform finite-difference grid of grid size $h = L/N$, where $N + 1$ is the number of grid points in each of the three coordinate directions. We approximate the values of the vector field $D = (D^1, D^2, D^3)$ at the grid points labeled by (i, j, k) by $(\hat{D}^1_{i,j,k}, \hat{D}^2_{i,j,k}, \hat{D}^3_{i,j,k})$, where $i, j, k = 0, 1, \ldots, N$. We use the central differencing scheme to discretize the partial derivatives of all the components of D at all the grid points, and use the trapezoidal numerical quadrature rule to approximate the integral $J[D]$ as iterated one-dimensional integrals. As a result, we obtain a $3(N + 1)^3$-variable convex function $\hat{J} = \hat{J}[\hat{D}]$ with $\hat{D} \in \mathbb{R}^{3(N+1)^3}$ the vector of components $\hat{D}^1_{i,j,k}$, $\hat{D}^2_{i,j,k}$, and $\hat{D}^3_{i,j,k}$ $(i, j, k = 0, 1, \ldots, N)$ in certain order. The gradient vector $\nabla\hat{J}[\hat{D}] \in \mathbb{R}^{3(N+1)^3}$ is calculated.

We use the gradient descent method with line search to minimize the convex function $\hat{J} = \hat{J}[\hat{D}]$. This iterative process begins with an initial displacement $\hat{D}_0 = (\hat{D}^1_0, \hat{D}^2_0, \hat{D}^3_0)$, and is terminated if the number of iteration reaches a given maximal number $k_{\max}$ or if the ℓ^2-norm of the gradient $\nabla\hat{J}$ at the current iterate $\hat{D}_k$ is smaller than a given tolerance δ_{T}. The step length in the line search is controlled by a shrinking parameter γ_{c}.

For our numerical tests, we set $\varepsilon = 1$ and $L = 1$, and define

$$\phi(x) = x_1(1 - x_1)\sin(\pi x_2)\sin(\pi x_3) \qquad \forall x = (x_1, x_2, x_3) \in \Omega = (0, 1)^3.$$

We then define $f = -\varepsilon\Delta\phi + B'(\phi)$ and $g = 0$ in Ω. Note that, with such f and g, the function ϕ is the solution to the PB equation (1.1) with the boundary condition $\phi = g$ on $\partial\Omega$, and the vector field $D := -\varepsilon\nabla\phi$ is the unique minimizer of the LTPB functional (1.3) over $H(\mathrm{div},\Omega)$. We also set $k_{\max} = 10^5$, $\delta_T = 10^{-7}$, and $\gamma_{\mathrm{c}} = 1/2$. The grid size is $h = 1/N$, where the value of N is varied in our tests. We consider two choices of the convex function B :

(1) $B(s) = s^2/2$. Its Legendre transform is $B^*(\xi) = \xi^2/2$;

(2) $B(s) = \cosh(s) - 1$. Direct calculations lead to $B^*(\xi) = 1 - \sqrt{\xi^2 + 1} + \xi \ln\left(\xi + \sqrt{\xi^2 + 1}\right)$.

For a fixed choice of B and an integer $N \geq 1$, we compute the numerical value of $\max I := I[\phi]$ by the finite difference and numerical quadrature. For $D = -\varepsilon\nabla\phi$, we have by the duality that $I[\phi] = J[D] = \min_{H(\mathrm{div},\Omega)} J$. We then use our algorithm described above to numerically minimize the functional J defined in (1.3). We denote by D_N the final numerical minimizer and by $\min J$ the final minimum value. We calculate the $L^2(\Omega)$-error, $\|D_N - D\|_{L^2(\Omega)}$, between D_N and the exact minimizer $D = -\varepsilon\nabla\phi$ of J, and the differences between the maximal value $\max I$ and the minimum value $\min J$.

Figure 1 shows the log-log plot of the L^2-error $\|D_N - D\|_{L^2(\Omega)}$ vs. the grid size $h = 1/N$ for both $B(s) = s^2/2$ and $B(s) = \cosh(s) - 1$. We observe that our method converges with the rate $O(h^{1.5})$. Figure 2 shows the log-log plot of the absolute value of the energy difference, $|\min J_N - \max I_N|$, vs. the grid size $h = 1/N$, where $\min J_N$ is the numerical minimum value of $\hat{J}$ and $\max I_N$ is the numerical integration value of $I[\phi]$ with the grid size $h = 1/N$. The convergence rate is observed to be $O(h^{3.3})$. We see from our numerical results that our simple discretization, integration, and optimization methods produce numerical minimizers and minimum values that converge to the exact ones. The convergence of the energy error also validates the duality as stated in Theorem 2.2.

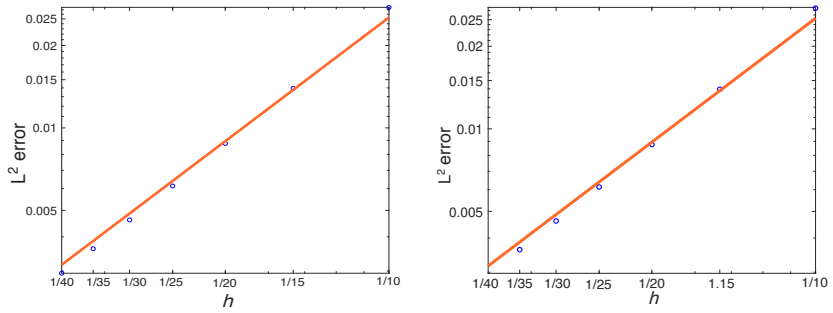

Figure 1: Log-log plot (circles) with linear fitting (straight line) of the L^2-error $\|D_N - D\|_{L^2(\Omega)}$ vs. the grid size $h = 1/N$ for $B(s) = s^2/2$ (left) and $B(s) = \cosh(s) - 1$ (right). Both straight lines have the slopt 1.5, indicating an $O(h^{1.5})$ convergence rate.

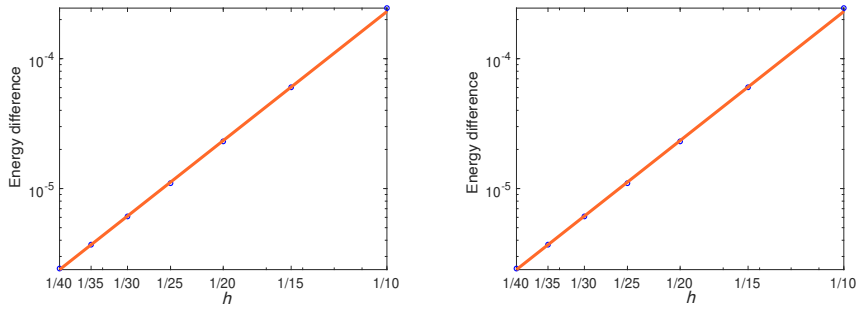

Figure 2: Log-log plot (circles) with linear fitting (straight line) of the absolute error $|\min J_N - \max I_N|$ (marked as "Energy difference") vs. the grid size $h = 1/N$ for $B(s) = s^2/2$ (left) and $B(s) = \cosh(s) - 1$ (right). Both straight lines have the slop 3.3, indicating an $O(h^{3.3})$ convergence rate.

3 A Penalty Method for LTPB Electrostatics with a Dielectric Boundary

3.1 A brief review of the theory

Let $\Omega \subset \mathbb{R}^3$ be a bounded domain with a Lipschitz-continuous boundary. Let Γ be a C^2, closed surface such that $\Gamma \subset \Omega$. Denote Ω_- the interior of Γ and $\Omega_+ = \Omega \setminus \overline{\Omega_-}$. Note that both Ω_- and Ω_+ are bounded open sets in $\mathbb{R}^3$, and $\Omega = \Omega_- \cup \Omega_+ \cup \Gamma$. Let $\varepsilon_- > 0$ and $\varepsilon_+ > 0$ be the distinct dielectric constants for Ω_- and Ω_+, respectively. We define the dielectric coefficient $\varepsilon_\Gamma : \Omega \to \mathbb{R}$ by

$$\varepsilon_\Gamma(x) = \begin{cases} \varepsilon_- & \text{if } x \in \Omega_-, \\ \varepsilon_+ & \text{if } x \in \Omega_+. \end{cases} \tag{3.1}$$

Let again $f \in L^2(\Omega)$ and $g \in H^1(\Omega)$. We define the set $H_g^1(\Omega)$ by (2.1) and the functional $I_\Gamma : H_g^1(\Omega) \cup \{-\infty\}$ by (1.5). This is the classical PB electrostatic energy applied to the molecular solvation with a continuum solvent [1, 4, 8, 11, 12, 14, 15, 25, 27]. The functional I_Γ is strictly concave downward and its extremization leads to the boundary-value problem of the PB equation

$$\begin{cases} \nabla \cdot \varepsilon_\Gamma \nabla \phi - \chi_+ B'(\phi) = -f & \text{in } \Omega, \\ \phi = g & \text{on } \partial\Omega. \end{cases} \tag{3.2}$$

Equivalently [20, 32],

$$\begin{cases} \varepsilon_- \Delta\phi = -f & \text{in } \Omega_-, \\ \varepsilon_+ \Delta\phi - B'(\phi) = -f & \text{in } \Omega_+, \\ [\![\phi]\!] = [\![\varepsilon_\Gamma \nabla\phi \cdot n]\!] = 0 & \text{on } \Gamma, \\ \phi = g & \text{on } \partial\Omega. \end{cases} \tag{3.3}$$

Here and below, $[\![u]\!] = u|_{\Omega_+} - u|_{\Omega_-}$ denotes the jump across Γ of a function $u : \Omega \to \mathbb{R}$ from Ω_+ to Ω_-, and n denotes the unit normal at Γ pointing from Ω_- to Ω_+.

The following theorem collects some useful results proved in [7, 14, 15, 18]:

Theorem 3.1 ([7, 14, 15, 18]). (1) *There exists a unique* $\phi_\Gamma = \arg\max_{\phi \in \mathrm{H}^1_{\mathrm{g}}(\Omega)} \mathrm{I}_\Gamma[\phi]$. *Moreover,* $\phi_\Gamma \in L^\infty(\Omega)$, *and there exists* $C > 0$, *independent of* Γ, *such that* $\|\phi_\Gamma\|_{H^1(\Omega)} + \|\phi_\Gamma\|_{L^\infty(\Omega)} \le C$.

(2) *If* $\partial\Omega$ *is smooth, then the maximizer* ϕ_Γ *satisfies* $\phi_\Gamma|_{\Omega_-} \in H^2(\Omega_-)$ *and* $\phi_\Gamma|_{\Omega_+} \in H^2(\Omega_+)$. *Moreover, it is the unique solution to the problem* (3.2) *and the problem* (3.3).

We consider minimizing the LTPB functional $J_\Gamma : V_\Gamma \to \mathbb{R} \cup \{+\infty\}$ defined by (1.4), where

$$V_\Gamma = \{D \in H(\mathrm{div}, \Omega) : \nabla \cdot D = f \text{ a.e. } \Omega_-\}.$$

Note that the set V_Γ is a convex subset of $H(\mathrm{div}, \Omega)$ and the functional J_Γ is strictly convex. By formal calculations, we obtain the Euler–Lagrange equation for the minimizer D_Γ [6]

$$\begin{cases} \nabla \cdot D_\Gamma = f & \text{in } \Omega_-, \\ \dfrac{D_\Gamma}{\varepsilon_+} + \nabla \left(B^{*\prime}(f - \nabla \cdot D_\Gamma) \right) = 0 & \text{in } \Omega_+, \\ [\![D_\Gamma \cdot n]\!] = 0 & \text{on } \Gamma, \\ \dfrac{1}{\varepsilon_-} D_\Gamma|_{\Omega_-} \cdot \tau = -\partial_\tau \left(B^{*\prime}(f - \nabla \cdot D_\Gamma)|_{\Omega_+} \right) & \text{on } \Gamma, \\ B^{*\prime}(f - \nabla \cdot D_\Gamma) = g & \text{on } \partial\Omega, \end{cases} \tag{3.4}$$

where τ is any unit vector tangential to Γ.

The LTPB formulation (i.e., the minimization of J_Γ over V_Γ) and the classical PB formulation (i.e., the maximization of I_Γ over $H^1_g(\Omega)$) are a pair of dual variational problems. The following theorem, proved in [6], provides both the week and strong dualities:

Theorem 3.2 ([6]). (1) *Weak duality. We have* $I_\Gamma[\phi] \le J_\Gamma[D]$ *for all* $\phi \in H^1_g(\Omega)$ *and all* $D \in V_\Gamma$.

(2) *Strong duality. Let* $D_\Gamma = -\varepsilon_\Gamma \nabla\phi_\Gamma$, *where* $\phi_\Gamma = \arg\max_{H^1_g(\Omega)} I_\Gamma$. *Then,* $D_\Gamma \in V_\Gamma$ *and* D_Γ *is the unique minimizer of* $J_\Gamma : V_\Gamma \to \mathbb{R} \cup \{+\infty\}$. *Moreover,* $J_\Gamma[D_\Gamma] = I_\Gamma[\phi_\Gamma]$.

3.2 A penalty method and its convergence

Since the Euler–Lagrange equation (3.4) for the minimizer D_Γ of the LTPB functional $J_\Gamma : V_\Gamma \to \mathbb{R} \cup \{+\infty\}$ is rather complicated, we propose to numerically minimize the functional J_Γ over V_Γ. To treat the constraint $\nabla \cdot D = f$ for all $D \in V_\Gamma$, we propose to use a penalty method: approximate the functional J_Γ by adding a penalty term, and minimize the resulting, penalized functional without the constraint. Specifically, we define the penalized functional $J_{\Gamma,\mu} : H(\mathrm{div}, \Omega) \to \mathbb{R} \cup \{+\infty\}$ for any $\mu > 0$, a penalty parameter, by

$$J_{\Gamma,\mu}[D] = J_\Gamma[D] + \frac{1}{2\mu} \int_{\Omega_-} (\nabla \cdot D - f)^2 \, dx$$

$$= \int_\Omega \left[\frac{1}{2\varepsilon_\Gamma}|D|^2 + \chi_+ B^*(f - \nabla\cdot D) + \frac{\chi_-}{2\mu}(\nabla\cdot D - f)^2 \right] dx + \int_{\partial\Omega} gD\cdot n\, dS, \tag{3.5}$$

where χ_+ and χ_- are the characteristic functions of Ω_+ and Ω_-, respectively. Clearly,

$$J_{\Gamma,\mu_1}[D] \geq J_{\Gamma,\mu_2}[D] \quad \forall D \in H^1(\mathrm{div},\Omega), \qquad \text{if } 0 < \mu_1 < \mu_2. \tag{3.6}$$

To prove the convergence of the penalized LTPB electrostatics in the limit $\mu \to 0$ and to compare different formulations, we define the corresponding, penalized PB functional $I_{\Gamma,\mu} : H^1_g(\Omega) \to \mathbb{R}\cup\{-\infty\}$ of electrostatic potentials by

$$\begin{aligned} I_{\Gamma,\mu}[\phi] &= I_\Gamma[\phi] - \frac{\mu}{2}\int_{\Omega_-} \phi^2\, dx \\ &= \int_\Omega \left[-\frac{\varepsilon_\Gamma}{2}|\nabla\phi|^2 + f\phi - \chi_+ B(\phi) - \frac{\chi_-\mu}{2}\phi^2 \right] dx \qquad \forall \phi \in H^1_g(\Omega). \end{aligned} \tag{3.7}$$

We note that the Legendre transform of the function $s \mapsto \mu s^2/2$ is $\xi \mapsto \xi^2/(2\mu)$.

The following theorem shows the convergence of the minimizers and minimum values of the penalized functionals $I_{\Gamma,\mu}$ to those of the non-penalized functional I_Γ:

Theorem 3.3. (1) *Let $\mu > 0$. There exists a unique $\phi_{\Gamma,\mu} = \arg\max_{\phi\in \mathrm{H}^1_{\mathrm{g}}(\Omega)} \mathrm{I}_{\Gamma,\mu}[\phi]$. Moreover, $\phi_{\Gamma,\mu} \in L^\infty(\Omega)$, and it is the unique weak solution in $H^1_g(\Omega)$ to the Euler–Lagrange equation*

$$-\nabla\cdot\varepsilon_\Gamma\nabla\phi_{\Gamma,\mu} + \chi_+ B'(\phi_{\Gamma,\mu}) + \mu\chi_-\phi_{\Gamma,\mu} = f \qquad \text{in } \Omega.$$

(2) *If $\phi_\Gamma = \arg\max_{\phi\in \mathrm{H}^1_{\mathrm{g}}(\Omega)} \mathrm{I}_\Gamma[\phi]$, then $\phi_{\Gamma,\mu} \to \phi_\Gamma$ in $H^1(\Omega)$ and $I_{\Gamma,\mu}[\phi_{\Gamma,\mu}] \to I_\Gamma[\phi_\Gamma]$ as $\mu \to 0$.*

Proof. (1) This is the same as the proof for the non-penalized functional ($\mu = 0$). The existence of a minimizer is obtained by the direct method in the calculus of variations. The regularity $\phi_{\Gamma,\mu} \in L^\infty(\Omega)$ follows from a comparison argument. This regularity is needed to obtain the Euler–Lagrange equation by the definition. See more details in [15].

(2) It suffices to show that for any sequence $\mu_k \searrow 0$, there is a subsequence, not relabelled, such that $\phi_{\Gamma,\mu_k} \to \phi_\Gamma$ in $H^1(\Omega)$ and $I_{\Gamma,\mu_k}[\phi_{\Gamma,\mu_k}] \to I_\Gamma[\phi_\Gamma]$ as $k \to \infty$.

First, we need some bound for all the maximizers $\phi_{\Gamma,\mu}$ ($\mu > 0$). Let $\hat{g} \in H^1_g(\Omega)$ be such that $\hat{g} = 0$ in Ω_-. We have for any $\mu > 0$ that $I_{\Gamma,\mu}[\phi_{\Gamma,\mu}] = \max_{\phi\in H^1_g(\Omega)} I_{\Gamma,\mu}[\phi] \geq I_{\Gamma,\mu}[\hat{g}] = I_\Gamma[\hat{g}] > -\infty$. It then follows from the definition of $I_{\Gamma,\mu}$ and Poincaré's inequality that

$$\sup_{\mu>0} \|\phi_{\Gamma,\mu}\|_{H^1(\Omega)} < \infty. \tag{3.8}$$

Now for any sequence $\mu_k \searrow 0$, by the above bound, there exists a subsequence of $\{\phi_{\Gamma,\mu_k}\}$, not relabelled, and some $\hat{\phi}_\Gamma \in H^1(\Omega)$ such that $\phi_{\Gamma,\mu_k} \rightharpoonup \hat{\phi}_\Gamma$ in $H^1(\Omega)$. But $H^1_g(\Omega)$ is convex and closed, and hence weakly closed in $H^1(\Omega)$. Thus, $\hat{\phi}_\Gamma \in H^1_g(\Omega)$. The convexity of $-I_\Gamma$ leads to

$$\limsup_{k\to\infty} I_\Gamma[\phi_{\Gamma,\mu_k}] \leq I_\Gamma[\hat{\phi}_\Gamma]. \tag{3.9}$$

We claim that $\hat{\phi}_\Gamma = \phi_\Gamma$, which is the maximizer of I_Γ over $H^1_g(\Omega)$. In fact, for each $k \geq 1$, $I_{\Gamma,\mu_k}[\phi_\Gamma] \leq I_{\Gamma,\mu_k}[\phi_{\Gamma,\mu_k}] \leq I_\Gamma[\phi_{\Gamma,\mu_k}]$. This and (3.9) imply that

$$\begin{aligned} I_\Gamma[\phi_\Gamma] &= \lim_{k\to\infty} I_{\Gamma,\mu_k}[\phi_\Gamma] \leq \liminf_{k\to\infty} I_{\Gamma,\mu_k}[\phi_{\Gamma,\mu_k}] \leq \liminf_{k\to\infty} I_\Gamma[\phi_{\Gamma,\mu_k}] \\ &\leq \limsup_{k\to\infty} I_\Gamma[\phi_{\Gamma,\mu_k}] \leq I_\Gamma[\hat{\phi}_\Gamma] \leq I_\Gamma[\phi_\Gamma]. \end{aligned} \tag{3.10}$$

Thus, $I_\Gamma[\hat{\phi}_\Gamma] = I_\Gamma[\phi_\Gamma]$, and $\hat{\phi}_\Gamma = \phi_\Gamma$ by the uniqueness of the maximizer of I_Γ. The combination of (3.9) and (3.10) now implies $I_{\Gamma,\mu_k}[\phi_{\Gamma,\mu_k}] \to I_\Gamma[\phi_\Gamma]$ as $k \to \infty$.

We prove finally the strong convergence $\phi_{\Gamma,\mu} \to \phi_\Gamma$ in $H^1(\Omega)$. Denote for each $k \geq 1$

$$a_k = \int_\Omega \Big[\frac{\varepsilon_\Gamma}{2}|\nabla\phi_{\Gamma,\mu_k}|^2 - \frac{\varepsilon_\Gamma}{2}|\nabla\phi_\Gamma|^2\Big]\,dx \quad \text{and} \quad b_k = \int_{\Omega_+} [B(\phi_{\Gamma,\mu_k}) - B(\phi_\Gamma)]\,dx.$$

Passing to a further subsequence if necessary, we have by the weak convergence $\phi_{\Gamma,\mu_k} \rightharpoonup \phi_\Gamma$ in $H^1(\Omega)$ that $\phi_{\Gamma,\mu_k} \to \phi_\Gamma$ in $L^2(\Omega)$ and $\phi_{\Gamma,\mu_k} \to \phi_\Gamma$ a.e. in Ω. These, together with the energy convergence $I_{\Gamma,\mu_k}[\phi_{\Gamma,\mu_k}] \to I_\Gamma[\phi_\Gamma]$ as $k \to \infty$ and the bound (3.8), imply that $a_k + b_k \to 0$ as $k \to \infty$. But $\liminf_{k\to\infty} a_k \geq 0$ as $\phi_{\Gamma,\mu_k} \rightharpoonup \phi_\Gamma$ in $H^1(\Omega)$ and $\liminf_{k\to\infty} b_k \geq 0$ by Fatou's lemma. Therefore,

$$0 = \lim_{k\to\infty}(a_k + b_k) \geq \liminf_{k\to\infty} a_k + \liminf_{k\to\infty} b_k \geq 0.$$

Hence $\liminf_{k\to\infty} a_k = 0$. Passing to a further subsequence if necessary and without relabelling, we have $a_k \to 0$ as $k \to \infty$. This and the weak convergence $\phi_{\Gamma,\mu_k} \rightharpoonup \phi_\Gamma$ in $H^1(\Omega)$, together with the identity

$$\|\nabla\phi_{\Gamma,\mu} - \nabla\phi_\Gamma\|^2 = \|\nabla\phi_{\Gamma,\mu}\|^2 - \|\nabla\phi_\Gamma\|^2 - \int_\Omega 2\nabla\phi_\Gamma \cdot \nabla(\phi_{\Gamma,\mu} - \phi_\Gamma)\,dx,$$

implty that $\nabla\phi_{\Gamma,\mu_k} \to \nabla\phi_\Gamma$ in $L^2(\Omega)$ and consequently that $\phi_{\Gamma,\mu} \to \phi_\Gamma$ in $H^1(\Omega)$. □

The following theorem provides the duality properties for the penalized functionals $I_{\Gamma,\mu}$ and $J_{\Gamma,\mu}$, its proof is similar to that of of Theorem 3.2 (cf. [6]), and is therefore omitted:

Theorem 3.4. *Let $\mu > 0$.*

(1) Weak duality. *We have $I_{\Gamma,\mu}[\phi] \leq J_{\Gamma,\mu}[D]$ for any $\phi \in H^1_g(\Omega)$ and any $D \in H(\mathrm{div},\Omega)$.*
(2) Strong duality. *Let $\phi_{\Gamma,\mu} = \arg\max_{\mathrm{H}^1_{\mathrm{g}}(\Omega)} \mathrm{I}_{\Gamma,\mu}$. Then, $D_{\Gamma,\mu} := -\varepsilon_\Gamma\nabla\phi_{\Gamma,\mu} \in H(\mathrm{div},\Omega)$ and $D_{\Gamma,\mu}$ is the unique minimizer of $J_{\Gamma,\mu} : H(\mathrm{div},\Omega) \to \mathbb{R}\cup\{+\infty\}$. Moreover, $J_{\Gamma,\mu}[D_{\Gamma,\mu}] = I_{\Gamma,\mu}[\phi_{\Gamma,\mu}]$.* □

The above two theorems, together with (3.6), imply immediately the following:

Theorem 3.5. *We have $D_{\Gamma,\mu} \to D_\Gamma$ in $H(\mathrm{div},\Omega)$. Moreover, as $\mu > 0$ decreases to 0, the minimum value $J_{\Gamma,\mu}[D_{\Gamma,\mu}] = \min_{D\in H^1(\mathrm{div},\Omega)} J_{\Gamma,\mu}[D]$ increases and converges to $J_\Gamma[D_\Gamma] = \min_{D\in V_\Gamma} J_\Gamma[D]$.* □

3.3 Numerical methods and tests

We choose $\Omega = (-L, L)^3$ for some $L > 0$ and cover $\overline{\Omega} = [-L, L]^3$ with a uniform finite-difference grid of grid size $h = 2L/N$, where $N+1$ is the number of grid points in each of the three coordinate directions. We approximate the values of a scalar function ϕ and a vector-valued function $D = (D^1, D^2, D^3)$ at the grid points labeled by (i, j, k) by $\hat{\phi}_{i,j,k}$ and $(\hat{D}^1_{i,j,k}, \hat{D}^2_{i,j,k}, \hat{D}^3_{i,j,k})$, respectively, where $i, j, k = 0, 1, \ldots, N$. We fix the parameters ε_- and ε_+, the functions $f \in L^2(\Omega)$ and $g \in H^1(\Omega)$, and a penalty parameter $\mu > 0$. As before, we consider again $B(s) = s^2/2$ and $B(s) = \cosh(s) - 1$.

We use the central differencing scheme to discretize partial derivatives of functions at all the grid points and the trapezoidal numerical quadrature rule to approximate the integrals $I_\Gamma[\phi]$, $I_{\Gamma,\mu}[\phi]$, and $J_{\Gamma,\mu}[D]$ as iterated one-dimensional integrals, respectively. After the discretization and numerical integration, we obtain the corresponding concave functions $\hat{I}_\Gamma$ and $\hat{I}_{\Gamma,\mu}$ of $\hat{\phi} \in \mathbb{R}^{(N-1)^3}$ with components $\hat{\phi}_{i,j,k}$ (for all $i, j, k \neq 0$ or N by the boundary condition $\phi = g$ on $\partial\Omega$), and a convex function $\hat{J}_{\Gamma,\mu}$ of $\hat{D} \in \mathbb{R}^{3(N+1)^3}$ with components $(\hat{D}^1_{i,j,k}, \hat{D}^2_{i,j,k}, \hat{D}^3_{i,j,k})$ for all i, j, k. The gradient vectors $\nabla\hat{I}_\Gamma$, $\nabla\hat{I}_{\Gamma,\mu}$, and $\nabla\hat{J}_{\Gamma,\mu}$ are also calculated.

Since molecular modeling often leads to large-scale simulations, we use the efficient, limited-memory Broyden–Fletcher–Goldfarb–Shanno (BFGS) algorithm, a quasi-Newton optimization algorithm [10,

19, 24], to minimize the convex functions $-\hat{I}_\Gamma$ and $\hat{J}_{\Gamma,\mu}$. The optimization iteration is terminated if the number of iteration reaches a given maximal number or if the ℓ^2-norm of the gradient $\nabla\hat{I}_\Gamma$, $\nabla\hat{I}_{\Gamma,\mu}$, or $\nabla\hat{J}_{\Gamma,\mu}$ is smaller than a given torelance.

For numerical tests, we set $L = 1$, $\Omega = (-1, 1)^3$, $\Gamma = \{x \in \mathbb{R}^3 : |x| = \sqrt{2}/2\}$, $\varepsilon_- = 1$, $\varepsilon_+ = 80$, $f = 1$, and $g = 0$. We first maximize numerically the functional $I_\Gamma : H^1_g(\Omega) \to \mathbb{R} \cup \{-\infty\}$ defined by (1.5) with a very fine grid to obtain a numerical maximizer $\phi_{\text{exact}} \in H^1_g(\Omega)$. We denote $D_{\text{exact}} = -\varepsilon_\Gamma \nabla\phi_{\text{exact}}$, and use it as the "exact" solution for testing our methods. We then choose several values of N, with $N + 1$ the number of grid size along one coordinate direction, and several values of the penalty parameter μ. For each pair of chosen N and μ, we minimize numerically the functional $J_{\Gamma,\mu} : H(\text{div}, \Omega) \to \mathbb{R} \cup \{\infty\}$, defined in (1.4), to obtain a numerical minimizer $D_{\mu,N} \in H(\text{div}, \Omega)$ and an approximation, $J_{\min,\mu,N} := J_{\Gamma,\mu}[D_{\mu,N}]$, of the minimum value of the functional $J_{\Gamma,\mu}$ over $H(\text{div}, \Omega)$. To test how the original constraint $\nabla \cdot D = f$ in $\Omega_- = \{x \in \Omega : |x| < R\}$, we define the penalty error

$$\text{PE}(\mu, N) := \int_{\Omega_-} |\nabla \cdot D_{\mu,N} - f|^2 dx. \tag{3.11}$$

In Figure 3, we plot the L^2 relative error $\|D_{\mu,N} - D_{\text{exact}}\|_{L^2(\Omega)}/\|D_{\text{exact}}\|_{L^2(\Omega)}$ vs. N with $N + 1$ the number of grid points in one direction for several values of the penalty parameter μ and for the function $B(s) = s^2/2$ (Figure 3, left) and $B(s) = \cosh(s) - 1$ (Figure 3, right). We see that in general the approximation $D_{\mu,N}$ to D_{exact} is better for smaller $\mu > 0$ and large N. Moreover, for a fixed N, the relative error decreases as the penalty μ decreases. These results indicate the convergence of our penalty method and numerical algorithm.

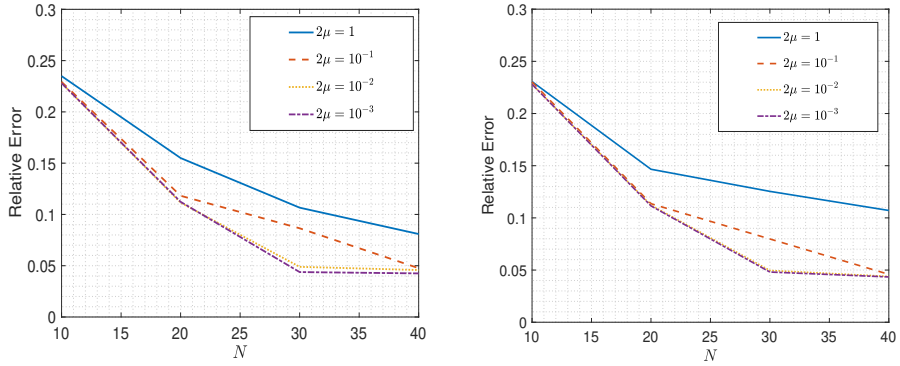

Figure 3: The L^2 relative error $\|D_{\mu,N} - D_{\text{exact}}\|_{L^2(\Omega)}/\|D_{\text{exact}}\|_{L^2(\Omega)}$ (marked as "Relative Error") vs. N with $N + 1$ the number of grid points in one coordinate direction. for $B(s) = s^2/2$ (left) and $B(s) = \cosh(s) - 1$ (right) for several μ-values.

In Figure 4, we show the log-log plot of the penalty error $\text{PE}(\mu, N)$ defined in (3.11) vs. $1/(2\mu)$ with μ the penalty parameter for several values of N and for both $B(s) = s^2/2$ and $B(s) = \cosh(s) - 1$. The slop of the lines are estimated to be close to -2. This indicates that $(1/\mu)\text{PE}(\mu, N) = O(\mu)$, and hence particularly,

$$\lim_{\mu\to 0^+} \frac{1}{2\mu} \int_{\Omega_-} |\nabla \cdot D_{\Gamma,\mu} - f|^2 \, dx = 0,$$

where $D_{\Gamma,\mu} = \arg\min_{H(\text{div},\Omega)} J_{\Gamma,\mu}$. This agrees with our convergence result that the minimum energy of $J_{\Gamma,\mu}$ over $H(\text{div}, \Omega)$ converges to that of J_Γ over V_T as $\mu \to 0$; cf. Theorem 3.5.

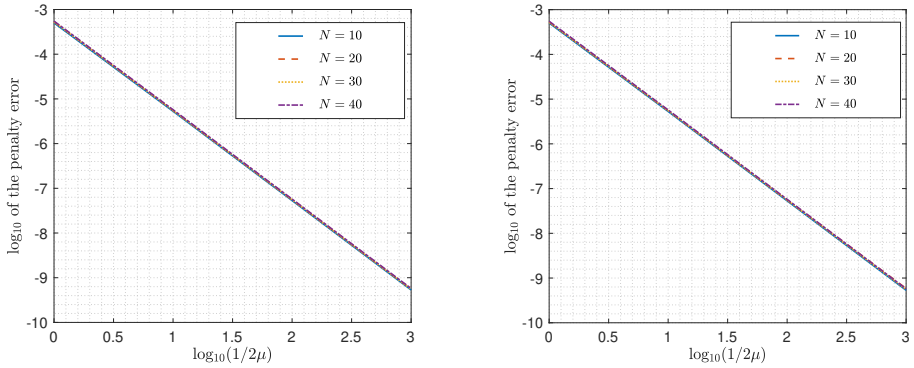

Figure 4: The log-log plot of the penalty error, defined in (3.11), vs. $1/(2\mu)$ with μ the penalty parameter for several values of N for $B(s) = s^2/2$ (left) and $B(s) = \cosh(s) - 1$ (right). The lines for different values of N almost overlap. The slope of these lines is close to -2.

4 Numerical Relaxation of a Dielectric Boundary and Comparison of the LTPB and PB Electrostatics

4.1 Gradient descent and boundary force

With the set up as in section 3, we now consider the minimization of the energy functional $G[\Gamma]$ of a boundary Γ defined in (1.6) that consists of both the surface energy and the electrostatic energy (1.7). The gradient descent iteration is a generic algorithm for minimizing the functional $G[\Gamma]$. Once Γ_k is given, the new boundary Γ_{k+1} is formally obtained by

$$\Gamma_{k+1} = \Gamma_k - \alpha_k \delta_\Gamma G[\Gamma_k],$$

i.e., a point $x_k \in \Gamma_k$ is moved to $x_{k+1} \in \Gamma_{k+1}$ by $x_{k+1} = x_k - \alpha_k \delta_\Gamma G[\Gamma_k](x_k)$. Here, $\alpha_k > 0$ is the step-size and $\delta_\Gamma G[\Gamma] : \Gamma \to \mathbb{R}$ is the first variation of $G[\Gamma]$ with respect to the perturbation of Γ. We shall call $-\delta_\Gamma G[\Gamma]$ the boundary force associated to the total energy $G[\Gamma]$.

The variation of the first part of the energy $G[\Gamma]$, the surface energy $\gamma_0 \mathrm{Area}\,(\Gamma)$, is $-2\gamma_0 H$, where H is the mean curvature. The variation of the electrostatic energy $E_{\mathrm{ele}}[\Gamma]$ (1.7) is given by [15, 18]

$$\delta_\Gamma E_{\mathrm{ele}}[\Gamma] = \frac{1}{2}\left(\frac{1}{\varepsilon_-} - \frac{1}{\varepsilon_+}\right)|\varepsilon_\Gamma \nabla\phi_\Gamma \cdot n|^2 + \frac{1}{2}(\varepsilon_+ - \varepsilon_-)\,|(I - n\otimes n)\nabla\phi_\Gamma|^2 + B(\phi_\Gamma) \quad \text{on } \Gamma, \tag{4.1}$$

where $\phi_\Gamma \in H^1_g(\Omega)$ is the unique maximizer of I_Γ over $H^1_g(\Omega)$ and I is the 3×3 identity matrix. It is noted that the force $-\delta_\Gamma E_{\mathrm{ele}}[\Gamma]$ always points from the lower to higher dielectric region; cf. [15]. By the duality, $D_\Gamma = -\varepsilon_\Gamma \nabla\phi_\Gamma$ is the unique minimizer of J_Γ over V_Γ, cf. Theorem 3.1 and Theorem 3.2. We have $\phi_\Gamma = B^{*\prime}(f - \nabla\cdot D_\Gamma)$ in Ω_+. This follows from the interface version of the Euler–Lagrange equation (3.3) for ϕ_Γ on Ω_+, $B'(\phi_\Gamma) = f - \nabla\cdot D_\Gamma = f + \varepsilon_+\Delta\phi_\Gamma$ in Ω_+, together with the property of the Legendre transform. Therefore, the variation $\delta_\Gamma E_{\mathrm{ele}}[\Gamma]$ can be also calculated by D_Γ as follows:

$$\begin{aligned}\delta_\Gamma E_{\mathrm{ele}}[\Gamma] = \frac{1}{2}\left(\frac{1}{\varepsilon_-} - \frac{1}{\varepsilon_+}\right)|D_\Gamma \cdot n|^2 + \frac{1}{2}(\varepsilon_+ - \varepsilon_-)\left|(I - n\otimes n)\frac{D_\Gamma}{\varepsilon_\Gamma}\right|^2 \\ + B\left(B^{*\prime}(f - \nabla\cdot D_\Gamma|_{\Omega_+})\right) \qquad \text{on } \Gamma.\end{aligned} \tag{4.2}$$

With our penalty method described in section 3, the electrostatic energy is approximated by

$$E_{\mathrm{ele},\mu}[\Gamma] := \min_{D\in H(\mathrm{div},\Omega)} J_{\Gamma,\mu}[D] = \max_{\phi\in H^1_g(\Omega)} I_{\Gamma,\mu}[\phi];$$

cf. Theorem 3.3 and Theorem 3.4. Let $\phi_{\Gamma,\mu} \in H^1_g(\Omega)$ be the unique maximizer of $I_{\Gamma,\mu}$ over $H^1_g(\Omega)$ and $D_{\Gamma,\mu} = -\varepsilon_\Gamma \nabla \phi_{\Gamma,\mu} \in H(\mathrm{div}, \Omega)$ the unique minimizer of $J_{\Gamma,\mu}$ over $H(\mathrm{div}, \Omega)$. By the same argument for obtaining the formula (4.1) and (4.2), we have

$$\begin{aligned}
\delta_\Gamma E_{\mathrm{ele},\mu}[\Gamma] = {} & \frac{1}{2}\left(\frac{1}{\varepsilon_-} - \frac{1}{\varepsilon_+}\right) |\varepsilon_\Gamma \nabla \phi_{\Gamma,\mu} \cdot n|^2 \\
& + \frac{1}{2}(\varepsilon_+ - \varepsilon_-) \left|(I - n \otimes n) \nabla \phi_{\Gamma,\mu}\right|^2 + B(\phi_{\Gamma,\mu}) - \frac{\mu}{2}\phi^2_{\Gamma,\mu} \qquad \text{on } \Gamma, \\
\delta_\Gamma E_{\mathrm{ele},\mu}[\Gamma] = {} & \frac{1}{2}\left(\frac{1}{\varepsilon_-} - \frac{1}{\varepsilon_+}\right) |D_{\Gamma,\mu} \cdot n|^2 + \frac{1}{2}(\varepsilon_+ - \varepsilon_-) \left|(I - n \otimes n)\frac{D_{\Gamma,\mu}}{\varepsilon_\Gamma}\right|^2 \\
& + B\left(B^{*\prime}(f - \nabla \cdot D_{\Gamma,\mu}|_{\Omega_+})\right) - \frac{1}{2\mu}\left(f - \nabla \cdot D_{\Gamma,\mu}|_{\Omega_-}\right)^2 \qquad \text{on } \Gamma.
\end{aligned}$$

To minimize the total energy $G[\Gamma]$ (1.6) with the PB electrostatic energy $E_{\mathrm{ele}}[\Gamma] = \max_{\phi \in H^1_g(\Omega)} I_\Gamma[\phi]$, we propose the following max-min algorithm with given Γ_k and ϕ_k:

The max-min algorithm. Given Γ_k and ϕ_k.

- Maximize I_{Γ_k} over $H^1_g(\Omega)$ by an iteration method with ϕ_k as the initial guess to obtain an approximate maximizer ϕ_{k+1};
- Use (4.1) to calculate $\delta_\Gamma E_{\mathrm{ele}}[\Gamma_k]$ using ϕ_{k+1} and then calculate $\delta_\Gamma G[\Gamma_k]$;
- Choose α_{k+1} and update $\Gamma_{k+1} = \Gamma_k - \alpha_{k+1}\delta_\Gamma G[\Gamma_k]$.

Similarly, to minimize the total energy $G[\Gamma]$ (1.6) with the LTPB electrostatic energy $E_{\mathrm{ele}}[\Gamma] = \min_{D \in V_T} J_\Gamma[D]$, we propose the following min-min algorithm with given Γ_k and D_k:

The min-min algorithm. Given Γ_k and D_k.

- Minimize J_{Γ_k} over V_{Γ_k} by an iteration method with D_k as the initial guess to obtain an approximate minimizer D_{k+1};
- Use (4.2) to calculate $\delta_\Gamma E_{\mathrm{ele}}[\Gamma_k]$ using D_{k+1} and then calculate $\delta_\Gamma G[\Gamma_k]$;
- Choose α_{k+1} and update $\Gamma_{k+1} = \Gamma_k - \alpha_{k+1}\delta_\Gamma G[\Gamma_k]$.

Algorithms for the penalty methods are similar, where we maximize $I_{\Gamma,\mu}$ instead of I_Γ over $H^1_g(\Omega)$ and minimize $J_{\Gamma,\mu}$ over $H(\mathrm{div}, \Omega)$ instead of minimizing J_Γ over V_Γ.

For large-scale simulations, it is desirable to have only a few iterations to get the approximate ϕ_{k+1} or D_{k+1}. It is of practical interest to see if the min-min algorithm is more stable than the max-min algorithm. We will study this issue for a model system.

4.2 A model spherical system

We consider a radially symmetric charged system such as a macroion centered at the origin. In this case, $\Omega_- = \{x \in \mathbb{R}^3 : |x| < R\}$, $\Omega_+ = \{x \in \mathbb{R}^3 : R < |x| < A\}$, and $\Gamma = \{x \in \mathbb{R}^3 : |x| = R\}$, where $A > 0$ and $R \in (0, A)$ are given constants. Denote $r = |x|$ for any $x \in \mathbb{R}^3$. The electrostatic potential ϕ is now a radially symmetric function, i.e., a function of r: $\phi = \phi(r)$. Since the electric displacement vector field D is proportional to $\nabla_x(\phi(r)) = \phi'(r)(x/r)$, we consider $D(x) = p(r)(x/r)$ with $p = p(r)$ a radially symmetric function. While such a vector filed is not radially symmetric, its Euclidean norm $|D(x)| = |p(r)|$ and divergence

$$\nabla \cdot D(x) = \frac{2}{r}p(r) + p'(r) = \frac{1}{r^2}(r^2 p(r))' \tag{4.3}$$

are radially symmetric. So, we shall consider the radially symmetric function $p = p(r)$ instead of the vector field $D(x)$. In order to get exact solutions (i.e., minimizers of penalized functionals), we consider the case $B(s) = (1/2)s^2$. Note that $B^*(\xi) = (1/2)\xi^2$.

We can now convert the functionals (1.5), (1.4), (3.7), and (3.5) in the cartesian coordinate into the functionals in the spherical coordinate, respectively,

$$I_R[\phi] = 4\pi \int_0^A \left(-\frac{\varepsilon_R}{2}|\phi'|^2 + f\phi - \frac{\chi_+}{2}\phi^2 \right) r^2 dr, \tag{4.4}$$

$$J_R[p] = 4\pi \int_0^A \left[\frac{1}{2\varepsilon_R} p^2 + \frac{\chi_+}{2} \left| f - \left(\frac{2}{r}p + p' \right) \right|^2 \right] r^2 dr + 4\pi g p(A) A^2. \tag{4.5}$$

$$I_{R,\mu}[\phi] = 4\pi \int_0^A \left(-\frac{\varepsilon_R}{2}|\phi'|^2 + f\phi - \frac{\chi_- \mu}{2}\phi^2 - \frac{\chi_+}{2}\phi^2 \right) r^2 dr, \tag{4.6}$$

$$J_{R,\mu}[p] = 4\pi \int_0^A \left[\frac{1}{2\varepsilon_R} p^2 + \frac{\chi_-}{2\mu} \left| f - \left(\frac{2}{r}p + p' \right) \right|^2 + \frac{\chi_+}{2} \left| f - \left(\frac{2}{r}p + p' \right) \right|^2 \right] r^2 dr + 4\pi g p(A) A^2. \tag{4.7}$$

Here, the dielectric coefficient $\varepsilon_R : [0, A] \to \mathbb{R}$ is given by $\varepsilon_R(r) = \varepsilon_-$ if $r < R$ and $\varepsilon_R(r) = \varepsilon_+$ if $r > R$, $f : [0, A] \to \mathbb{R}$ is a smooth function, $g \in \mathbb{R}$ is a given constant, χ_- and χ_+ are the characteristic functions of $(0, R)$ and (R, A), respectively, and $\mu > 0$ is the penalty parameter. Note that the radially symmetric electrostatic potential $\phi = \phi(r)$ and the radially symmetric electric displacement $p = p(r)$ are related by $p = -\varepsilon_R \phi'$.

We denote $\omega(r) = r^2$ and define the space of electrostatic potentials to be

$$H^1_\omega(0, A) = \{\phi : (0, A) \to \mathbb{R} : \text{weakly differentiable and } \int_0^A (\phi^2 + \phi'^2) r^2 dr < \infty\}.$$

It is a Hilbert space with the inner product and norm

$$\langle \phi, \psi \rangle_\omega = \int_0^A (\phi\psi + \phi'\psi') r^2 dr \quad \text{and} \quad \|\phi\|_\omega = \sqrt{\langle \phi, \phi \rangle_\omega},$$

respectively. Note that $I_R[\phi]$ and $I_{R,\mu}[\phi]$ are finite if $\phi \in H^1_\omega(0, A)$. We shall consider the maximization of the functionals $I_R[\phi]$ and $I_{R,\mu}[\phi]$ over the set of admissible electrostatic potentials

$$X = \{\phi \in H^1_\omega(0, A) : \phi(A) = g\}.$$

If $\phi \in H^1_\omega(0, A)$ and $0 < \delta < A$, then $\phi \in H^1(\delta, A)$ and hence ϕ is absolutely continuous on $[\delta, A]$. Hence, the trace $\phi(A)$ is well defined.

We also define the space of functions representing the electric displacements to be

$$Y = \left\{ p : (0, A) \to \mathbb{R} : \text{weakly differentiable and } \int_0^A [(r^2 p)^2 + ((r^2 p)')^2] \frac{1}{r^2} dr < \infty \right\}.$$

This is also a Hilbert space with the inner product and norm

$$\langle p, q \rangle_Y = \int_0^A \left[(r^2 p)(r^2 q) + (r^2 p)'(r^2 q)' \right] \frac{1}{r^2} dr \quad \text{and} \quad \|p\|_Y = \sqrt{\langle p, p \rangle_Y},$$

respectively. By expanding the integrand of the integral in the definition of Y, one can see that $Y = H^1_\omega(0, A) \cap L^2(0, A)$. Note that $J_R[p]$ and $J_{R,\mu}[p]$ are finite for each $p \in Y$; cf. (4.3). Note also that, if $p \in Y$, then $p \in H^1(\delta, A)$ for any $\delta \in (0, A)$, and hence the trace $p(A)$ is well defined. We shall consider the minimization of $J_{R,\mu}$ ($\mu > 0$) over the space Y and that of J_R over the subset Y_0 of Y defined by

$$Y_0 = \left\{ p \in Y : \frac{2}{r}p + p' = f \text{ in } (0, R) \right\}.$$

The equation in defining Y_0 is equivalent to $(r^2 p(r))' = r^2 f(r)$ for $0 < r < R$. This is the same as the constraint $\nabla \cdot D = f$ in Ω_- in the cartesian coordinates for $D(r) = p(r)(x/r)$.

We note that the results of analysis presented in Section 3 are not for the class of radially symmetric functions, even the regions Ω_- and Ω are spheres, and therefore do not apply directly to the spherical system we discuss here. For completeness, we present those results for our system in the following theorem, and give a brief proof of this theorem in Appendix:

Theorem 4.1. (1) *Denote $I_{R,0} = I_R$. For each $\mu \geq 0$, there exists a unique $\phi_{R,\mu} \in X$ such that $I_{R,\mu}[\phi_{R,\mu}] = \max_{\phi \in X} I_{R,\mu}[\phi]$. Moreover, $\phi_{R,\mu} \in X$ is the unique solution to*

$$\begin{cases} \varepsilon_- \dfrac{1}{r^2}(r^2\phi')' - \mu\phi = -f & \text{in } (0,R), \\ \varepsilon_+ \dfrac{1}{r^2}(r^2\phi')' - \phi = -f & \text{in } (R,A), \\ \varepsilon_- \phi'(R-) = \varepsilon_+ \phi'(R+), \\ \phi(A) = g. \end{cases}$$

(2) Duality. *We have $I_R[\phi] \leq J_R[p]$ for any $\phi \in X$ and $p \in Y_0$, and $I_{R,\mu}[\phi] \leq J_{R,\mu}[p]$ for any $\mu > 0$, $\phi \in X$, and $p \in Y$. Moreover, $p_R := -\varepsilon_R \phi_R \in Y_0$ and $p_{R,\mu} := -\varepsilon_R \phi_{R,\mu} \in Y$ $(\mu > 0)$ are the unique minimizers of J_R over Y_0 and $J_{R,\mu}$ over Y, respectively.*

(3) Convergence. *We have $\|\phi_{R,\mu} - \phi_R\|_\omega \to 0$, $\max_{\phi \in X} I_{R,\mu}[\phi] \to \max_{\phi \in X} I_R[\phi]$, $\|p_{R,\mu} - p_R\|_Y \to 0$, and $\min_{p \in Y} J_{R,\mu}[\phi] \to \min_{p \in Y_0} J_R[p]$ as $\mu \to 0$.*

The total energy $G[\Gamma]$ defined in (1.6) now converts to the total energy function

$$G(R) = 4\pi\gamma_0 R^2 + \max_{\phi \in X} I_R[\phi] = 4\pi\gamma_0 R^2 + \min_{p \in Y_0} J_R[p]. \tag{4.8}$$

The boundary variation of the surface energy $\gamma_0 \text{Area}(\Gamma)$ is $-2\gamma_0 H$, where H is the mean curvature. Therefore, by (4.1) and (4.2), the boundary variation of the total energy $G(R)$ as a functional of the spherical interface $\{x \in \mathbb{R}^3 : |x| = R\}$ is given by

$$\begin{aligned} \delta_R G(R) &= \frac{2\gamma_0}{R} + \frac{1}{2}\left(\frac{1}{\varepsilon_-} - \frac{1}{\varepsilon_+}\right)\left[\varepsilon_R \phi_R'(R)\right]^2 + \frac{1}{2}\left[\phi_R(R)\right]^2 \\ &= \frac{2\gamma_0}{R} + \frac{1}{2}\left(\frac{1}{\varepsilon_-} - \frac{1}{\varepsilon_+}\right)\left[p_R(R)\right]^2 + \frac{1}{2}\left[f(R) - p_R'(R+) - \frac{2}{R}p_R(R_+)\right]^2, \end{aligned}$$

where $\phi_R \in X$ is the unique maximizer of I_R over X and $p_R = -\varepsilon_R \phi_R' \in Y_0$ is the unique minimizer of J_R over Y_0. Note that the boundary variation $\delta_R G$ differs from the derivative $G'(R)$ by the factor $4\pi R^2$; cf. [4].

For $\mu > 0$, the penalized approximation of the total energy is

$$G_\mu(R) = 4\pi\gamma_0 R^2 + \max_{\phi \in X} I_{R,\mu}[\phi] = 4\pi\gamma_0 R^2 + \min_{p \in Y} J_{R,\mu}[p]. \tag{4.9}$$

The boundary variation is

$$\begin{aligned} \delta_R G_\mu(R) &= \frac{2\gamma_0}{R} + \frac{1}{2}\left(\frac{1}{\varepsilon_-} - \frac{1}{\varepsilon_+}\right)\left[\varepsilon_R \phi_{R,\mu}'(R)\right]^2 + \frac{(1-\mu)}{2}\left[\phi_{R,\mu}(R)\right]^2 \\ &= \frac{2\gamma_0}{R} + \frac{1}{2}\left(\frac{1}{\varepsilon_-} - \frac{1}{\varepsilon_+}\right)\left[p_{R,\mu}(R)\right]^2 + \frac{1}{2}\left[f(R) - p_{R,\mu}'(R+) - \frac{2}{R}p_{R,\mu}(R+)\right]^2 \\ &\quad - \frac{1}{2\mu}\left[f(R) - p_{R,\mu}'(R-) - \frac{2}{R}p_{R,\mu}(R-)\right]^2, \end{aligned}$$

where $\phi_{R,\mu} \in X$ is the unique maximizer of $I_{R,\mu}$ over X and $p_{R,\mu} = -\varepsilon_R \phi_{R,\mu}' \in Y$ is the unique minimizer of $J_{R,\mu}$ over Y.

4.3 Numerical methods and tests

We fix all the parameters and functions: $A > 0$, $R \in (0, A)$, γ_0, ε_-, ε_+, $f : [0, A] \to \mathbb{R}$, $g \in \mathbb{R}$, and μ_0. We only consider the case $B(s) = s^2/2$, as we mainly compare the min-min and max-min approaches. We cover $[0, A]$ with a uniform finite-difference grid of grid size $h = A/N$ with the grid points $r_i = ih$ $(i = 0, \ldots, N)$, and denote by $\hat{\phi}_i$ and $\hat{p}_i$ the approximation of $\phi(r_i)$ and $p(r_i)$, respectively. We discretize the derivatives using the central differencing scheme and approximate integrals using the trapezoidal rule to obtain a concave function $\hat{I}_{R,\mu} = \hat{I}_{R,\mu}(\hat{\phi}_0, \hat{\phi}_1, \ldots, \hat{\phi}_{N-1})$ approximating $I_{R,\mu}[\phi]$ and a convex function $\hat{J}_{R,\mu} = \hat{J}_{R,\mu}(\hat{p}_0, \hat{p}_1, \ldots, \hat{p}_N)$ approximating $J_{R,\mu}[\phi]$. Note that $\hat{\phi}_N$ is not a degree of freedom, since $\phi(A) = \phi(r_N) = A$ is given. We also calculate the gradient vectors $\nabla \hat{I}_{R,\mu}$ and $\nabla \hat{J}_{R,\mu}$.

We now report and analyze the results of our numerical tests. We first use the conjugate gradient method to minimize both the functionals $-I_{R,\mu}$ and $J_{R,\mu}$ for a fixed R and for various values of the penalty parameter μ and different numbers of the grid points N to test the duality as established in Theorem 4.1 and the convergence of our numerical algorithms. In these tests, $A = 1$, $R = 1/2$, $\varepsilon_- = 1$, $\varepsilon_+ = 80$, and $g = 5$. We consider two examples of the function f: $f(r) = 1$ and $f(r) = (1000/\sqrt{2\pi})e^{-50r^2}$. For each N, the corresponding numerical maximizers and minimizers are denoted by ϕ_N and p_N, respectively. In Figure 5, we plot the L^2-error $\|p_N - (-\varepsilon_R \phi_N')\|_{L^2(0,A)}$ and also the energy difference vs. the number of grid points N for several values of the penalty parameter μ. The energy difference is defined as the absolute value of the difference between the computed maximum value of $I_{R,\mu}$ and the computed minimum value of $J_{R,\mu}$. We see clearly that as N gets larger the L^2-error gets smaller, and the difference between the maximum of $I_{R,\mu}$ and minimum of $J_{R,\mu}$ gets smaller. Therefore, our numerical method and implementation correctly verified the duality.

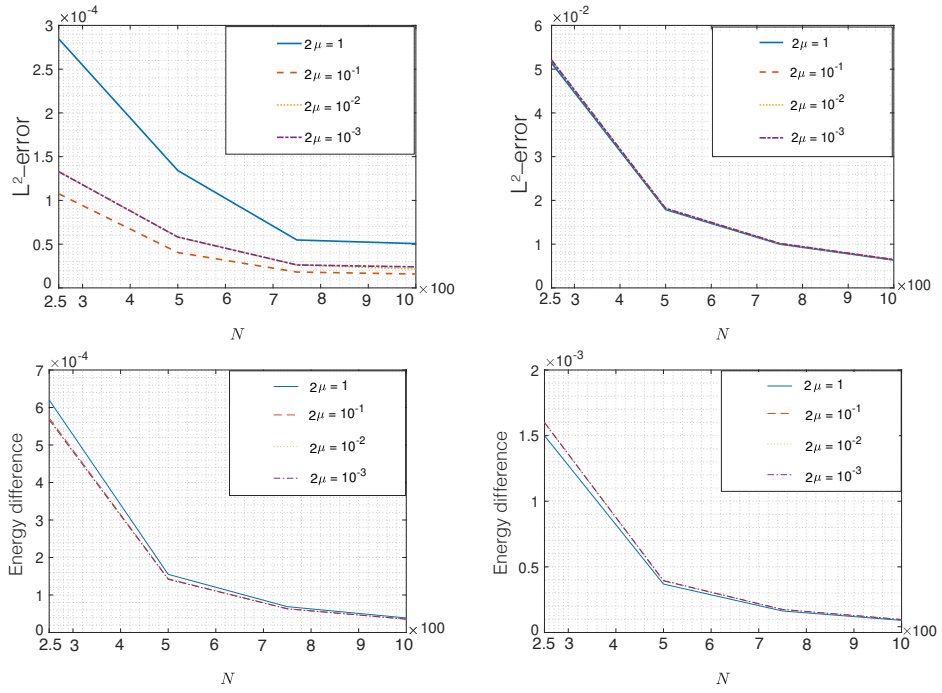

Figure 5: The L^2-error (upper panel) and the energy difference (lower panel) vs. the number of grid points N for $f(r) = 1$ (left) and $f(r) = (1000/\sqrt{2\pi})e^{-50r^2}$ (right) for several μ-values.

In Table 1, we show the time in seconds for each run of our code for numerically minimizing the functional $J_{R,\mu}$ and numerically maximizing the functional $I_{R,\mu}$ for several values of the penalty parameter μ and a fixed number of grid points $N = 1000$. We test both the function $f(r) = 1$ and $f(r) = (1000/\sqrt{2\pi})e^{-50r^2}$. We observe that in general the numerical minimization of $J_{R,\mu}$ and the

numerical maximization of $I_{R,\mu}$ have a similar efficiency. This is partially due to the underlying system is not very large. If the penalty value μ is not very small, then the minimization of $J_{R,\mu}$ is more efficient than that of the maximization of $I_{R,\mu}$. However, if the parameter μ is very small, then maximizing $I_{R,\mu}$ is faster than minimizing $J_{R,\mu}$. This may likely be due to the fact that the μ-term in $J_{R,\mu}$ makes the discretized and convex function relatively steep and the gradient is very large so that more steps are needed in the conjugate gradient iteration.

2μ	$f(r)=1$		$f(r)=(1000/\sqrt{2\pi})e^{-50r^2}$	
	min time	max time	min time	max time
10^{-1}	1	11	1	10
10^{-2}	2	10	1	10
10^{-3}	5	12	6	12
10^{-4}	10	11	10	12
10^{-5}	27	10	27	12

Table 1: Computational time in seconds for minimizing the functional $J_{R,\mu}$ (mark as "min time") and minimizing the functional $-I_{R,\mu}$ (marked as "max time") for several values of the penalty parameter μ and two different functions $f(r)$. The number of grid points is fixed to be $N = 1000$.

We now test the min-min and max-min approaches that are described in subsection 4.1 for minimizing the total energy $G_\mu = G_\mu(R)$ defined in (4.9) for a fixed μ. Note that the electrostatic part of the total energy $G_\mu(R)$ is defined by both $\min J_{R,\mu}$ and $\max I_{R,\mu}$. We minimize the total energy $G_\mu = G_\mu(R)$ using the gradient descent method. After we find some approximation of the radius R_k, then we maximize $I_{R_k,\mu}$ and minimize $J_{R_k,\mu}$ using the conjugate gradient descent method to find an approximate maximizer ϕ_{k+1} of $I_{R_k,\mu}$ and an approximate minimizer p_{k+1} of $J_{R_k,\mu}$. These approximate optimizers are then used to calculate the gradient $\nabla G(R_k)$. We use a relatively fewer steps in the conjugate gradient iterations for finding ϕ_{k+1} and p_{k+1} in the max-min and min-min algorithms, respectively, and compare the classical PB and the new LTPB formulations in terms of accuracy, efficiency, and stability of numerical computations.

We set $A = 1$, $\gamma_0 = 1$, $\varepsilon_- = 80$, $\varepsilon_+ = 1$, and $g = 1$. Note that $\varepsilon_- > \varepsilon_+$. This corresponds to an interesting molecular application where water molecules are burried in a large protein molecule; cf. the discussions and references in [5, 17]. We consider again the two functions $f : [0, A] \to \mathbb{R}$ given by $f(r) = 1$ and $f(r) = (1000/\sqrt{2\pi})e^{-50r^2}$. In order to compare the min-min and max-min algorithms, we first minimize the total energy function $G = G(R)$ defined in (4.8) that does not have the parameter μ. With the initial guess $R_0 = 1/\sqrt{2}$, the approximate (local) minimum value $G_{\min}$ and (local) minimizer $R_{\min}$ of G are found to be, respectively,

$$G_{\min} = 2.0944 \quad \text{and} \quad R_{\min} = 5.9325 \times 10^{-7} \qquad \text{for } f(r) = 1,$$
$$G_{\min} = 8.0605 \quad \text{and} \quad R_{\min} = 0.3710 \qquad \text{for } f(r) = \frac{1000}{\sqrt{2\pi}} e^{-50r^2}.$$

We choose a few values of the grid points N and a few values of the penalty parameter μ, and run our numerical computations with the min-min and max-min algorithms, respectively. In our gradient descent iteration for minimizing the function $G_\mu = G_\mu(R)$, we choose the initial guess to be $R_0 = 1/\sqrt{2}$, same as that used in minimizing $G = G(R)$. In Table 2 and Table 3, we show our numerical results for $f(r) = 1$ and $f(r) = (1000/\sqrt{2\pi})e^{-50r^2}$, respectively, and in each table, for $2\mu = 10^{-1}$ (upper), $2\mu = 10^{-3}$ (middel), and $2\mu = 10^{-5}$ (lower), respectively. In these tables, the "Step" means the number of steps in the conjugate gradient iteration for minimizing $J_{R,\mu}$ and $-I_{R,\mu}$. The "energy error" and "radius error" are the absolute error between the numerical minimum value of G_μ and $G_{\min}$ and that between the numerical approximation of a minimizer of G_μ and $R_{\min}$.

N	Step	min-min			min-max		
		energy error	radius error	time	energy error	radius error	time
250	20	0.0177	$9.9147 \cdot 10^{-8}$	1s	$1.2279 \cdot 10^{3}$	0.8940	1s
500	30	0.0800	$5.5155 \cdot 10^{-8}$	1s	$2.0281 \cdot 10^{3}$	0.8974	1s
750	40	0.0479	$2.8065 \cdot 10^{-8}$	1s	$1.8181 \cdot 10^{3}$	0.8453	1s
1000	50	0.0507	$1.8288 \cdot 10^{-7}$	1s	$2.3916 \cdot 10^{3}$	0.9119	2s

$f(r) = 1$ and $2\mu = 10^{-1}$.

N	Step	min-min			min-max		
		energy error	radius error	time	energy error	radius error	time
250	20	0.0226	$4.6575 \cdot 10^{-8}$	1s	854.8550	0.7007	1s
500	30	0.0664	$1.1507 \cdot 10^{-7}$	1s	$2.5794 \cdot 10^{3}$	0.9571	1s
750	50	0.0066	$1.0083 \cdot 10^{-7}$	1s	$1.8220 \cdot 10^{3}$	0.9980	1s
1000	50	0.0470	$2.9565 \cdot 10^{-7}$	1s	$2.3526 \cdot 10^{3}$	0.8957	2s

$f(r) = 1$ and $2\mu = 10^{-3}$.

N	Step	min-min			min-max		
		energy error	radius error	time	energy error	radius error	time
250	20	0.0613	$1.2250 \cdot 10^{-7}$	1s	$1.4453 \cdot 10^{3}$	0.9730	1s
500	30	0.0828	$1.1964 \cdot 10^{-7}$	1s	$1.1779 \cdot 10^{3}$	0.6993	1s
750	50	0.0578	$3.7498 \cdot 10^{-8}$	1s	$1.1117 \cdot 10^{3}$	0.9571	1s
1000	60	0.0607	$4.0233 \cdot 10^{-7}$	1s	$1.3643 \cdot 10^{3}$	0.8678	2s

$f(r) = 1$ and $2\mu = 10^{-5}$.

Table 2: Numerical results for $f(r) = 1$ and three μ-values. The "Step" means the number of steps in the conjugate gradient iteration for minimizing $J_{R,\mu}$ and $-I_{R,\mu}$. The "energy error" and "radius error" are the absolute error between the numerical minimum value of G_μ and $G_{\min}$ and that between the numerical approximation of a minimizer of G_μ and $R_{\min}$.

We observe from Table 2 and Table 3 that in general the min-min algorithm performs much better than the max-min algorithm in terms of the computational accuracy and efficency. As N increases, both the min-min and max-min algorithms take longer time to reach to the minimum value approximately. For the case $f(r) = 1$ with any of those μ-values and any of the number of grid points N, the min-min algorithm is more accurate and efficient than the max-min algorithm. With not so many Steps, the min-min algorithm produces good approximations of the minimum energy value $G_{\min}$ and the minimizer of $R_{\min}$, while the max-min algorithm produces the approximations with very large errors. For the case $f(r) = (1000/\sqrt{2\pi})e^{-50r^2}$ with a small but not so small value of μ, the min-min algorithm is still more accurate and efficient than the max-min algorithm. However, as μ decreases to 0, the max-min algorithm performs better than the min-min algorithm. Overall, our numerical results suggest that the min-min algorithm with a few numbers of Steps may be more accurate and efficient than the max-min algorithm in large-scale computations.

N	Step	min-min			min-max		
		energy error	radius error	time	energy error	radius error	time
250	150	0.0269	0.0050	1s	24.3156	0.3344	1s
500	300	0.0225	0.0010	1s	31.6441	0.3355	2s
750	500	0.0166	0.0078	1s	28.3402	0.3751	7s
1000	500	0.0189	0.0089	6s	38.4510	0.3360	27s

$f(r) = (1000/\sqrt{2\pi})e^{-50r^2}$ and $2\mu = 10^{-1}$.

N	Step	min-min			min-max		
		energy error	radius error	time	energy error	radius error	time
250	500	0.0178	0.0030	1s	1.8707	0.3039	3s
500	1000	0.0043	0.0030	3s	2.0348	0.3351	8s
750	1200	0.0058	0.0110	7s	12.8557	0.3372	14s
1000	1500	0.0048	0.0060	24s	13.8456	0.4194	41s

$f(r) = (1000/\sqrt{2\pi})e^{-50r^2}$ and $2\mu = 10^{-3}$.

N	Step	min-min			min-max		
		energy error	radius error	time	energy error	radius error	time
250	700	0.0159	0.0107	7s	0.0169	0.0030	2s
500	1600	0.0088	0.0090	32s	0.0092	0.0070	7s
750	2500	0.0050	0.0096	77s	0.0060	0.0057	12s
1000	3000	0.0016	0.0109	402s	0.0046	0.0060	40s

$f(r) = (1000/\sqrt{2\pi})e^{-50r^2}$ and $2\mu = 10^{-5}$.

Table 3: Numerical results for $f(r) = (1000/\sqrt{2\pi})e^{-50r^2}$ and three μ-values. The "Step" means the number of steps in the conjugate gradient iteration for minimizing $J_{R,\mu}$ and $-I_{R,\mu}$. The "energy error" and "radius error" are the absolute error between the numerical minimum value of G_μ and $G_{\min}$ and that between the numerical approximation of a minimizer of G_μ and $R_{\min}$.

Appendix

To prove Theorem 4.1, we need the following lemma that summarizes some properties, particularly the behavior near $r = 0$, of the functions in $H^1_\omega(0, A)$ and Y defined in section 4:

Lemma A.1. *Let $\phi \in H^1_\omega(0, A)$ and $p \in Y$. Define $u(r) = r^2 p(r)$ and $v(r) = r^2\phi(r)p(r)$ for $0 < r \le A$. Then, $\sup_{0<r<A} \sqrt{r}|\phi(r)| < \infty$, $u \in H^1(0, A)$ and $u(r) = o(r^{3/2})$ as $r \to 0$, and $v \in W^{1,1}(0, A)$ and $v(r) = o(r)$ as $r \to 0$.*

Proof. Note for any $\delta \in (0, A)$ that $\phi \in H^1(\delta, A)$ and hence ϕ is absolutely continuous on $[\delta, A]$. Now for any $r \in (0, A)$, we have

$$\begin{aligned}\phi(r)^2 &= \left[\phi(A) - \int_r^A \phi'(s)\, ds\right]^2 \\ &\le 2\phi(A)^2 + 2\left(\int_r^A \phi'(s) ds\right)^2\end{aligned}$$

$$\le 2\phi(A)^2 + 2\left(\int_r^A s^2\phi'(s)^2 ds\right)\left(\int_r^A s^{-2} ds\right)$$
$$= 2\phi(A)^2 + 2\left(\int_r^A s^2\phi'(s)^2 ds\right)\left(\frac{1}{r} - \frac{1}{A}\right)$$
$$\le 2\phi(A)^2 + \frac{2}{r}\|\phi\|_\omega^2.$$

Consequently, $r\phi(r)^2 \le 2A\phi(A)^2 + 2\|\phi\|^2_{H^1_\omega(0,A)}$, and hence $\sup_{0<r<A}\sqrt{r}|\phi(r)| < \infty$.

Since $p \in Y$, we can directly verify that $u \in H^1(0,A)$, and hence u is absolutely continuous on $[0,A]$. We must have $u(0) := \lim_{r\to 0} u(r) = 0$, since

$$\int_0^A \frac{u(r)^2}{r^2} dr = \int_0^A r^2 p(r)^2 dr < \infty.$$

Consequently, we have for $0 < r < A$ that

$$u(r)^2 = \left(\int_0^r u'(s)\, ds\right)^2 \le \left(\int_0^r s^2 ds\right)\left(\int_0^r \frac{u'(s)^2}{s^2} ds\right) = \frac{1}{3} r^3\, o(1) \qquad \text{as } r \to 0,$$

and hence $u(r) = o(r^{3/2})$ as $r \to 0$.

Since $v(r) = r^2\phi(r)p(r)$ $(0 < r < A)$, we have $\|v\|_{L^1(0,A)} \le \|\phi\|_\omega \|p\|_Y < \infty$. Consequently,

$$\int_0^A |v'(r)| dr = \int_0^A |\phi'(r) r^2 p(r) + \phi(r)(r^2 p(r))'| dr$$
$$\le \int_0^A |r\phi'(r)\, rp(r)| dr + \int_0^A \left| r\phi(r)\, \frac{[r^2 p(r)]'}{r} \right| dr$$
$$\le \left(\int_0^A r^2\phi'(r)^2 dr\right)^{1/2}\left(\int_0^A r^2 p(r)^2 dr\right)^{1/2}$$
$$+ \left(\int_0^A r^2\phi(r)^2 dr\right)^{1/2}\left(\int_0^A [(r^2 p(r))']^2 \frac{1}{r^2} dr\right)^{1/2}$$
$$\le 2\|\phi\|_\omega \|p\|_Y < \infty.$$

Hence, $v \in W^{1,1}(0,A)$, it is absolutely continuous, and $v(r) = \sqrt{r}\phi(r)u(r)/\sqrt{r} = o(r)$ as $r \to 0$. □

We now prove briefly Theorem 4.1 by providing mainly some details related to the properties of functions in $H^1_\omega(0,A)$ and Y, respectively.

Proof of Theorem 4.1. (1) This part can be proved using the direct method in the calculus of variations; cf. [14, 15, 18].

(2) Let $\mu > 0$, $\phi \in X$, and $p \in Y$. Since $\phi(A) = g$ and $\lim_{r\to 0^+} r^2\phi(r)p(r) = 0$ by Lemma A.1,

$$\int_0^A p\phi' r^2 dr = -\int_0^A \left(r^2 p\right)' \phi dr + gp(A)A^2 = -\int_0^A \left(\frac{2}{r}p + p'\right)\phi r^2 dr + gp(A)A^2.$$

Consequently, by the fact that the Legendre transform of $s \mapsto (\mu/2)s^2$ is $\xi \mapsto \xi^2/(2\mu)$, we obtain

$$I_{R,\mu}[\phi] \le I_{R,\mu}[\phi] + 4\pi \int_0^A \frac{1}{2\varepsilon_R}|p + \varepsilon_R\phi'|^2 r^2\, dr$$
$$= 4\pi \int_0^A \left(f\phi - \frac{\chi_- - \mu}{2}\phi^2 - \frac{\chi_+}{2}\phi^2 + \frac{1}{2\varepsilon_R}p^2 + p\phi'\right) r^2 dr.$$

$$
\begin{aligned}
&= 4\pi \int_0^A \left\{ \frac{1}{2\varepsilon_R} p^2 + \chi_- \left[\left(f - \left(\frac{2}{r} p + p' \right) \right) \phi - \frac{\mu}{2} \phi^2 \right] \right. \\
&\qquad \left. + \chi_+ \left[\left(f - \left(\frac{2}{r} p + p' \right) \right) \phi - \frac{\phi^2}{2} \right] \right\} r^2 dr + 4\pi g p(A) A^2 \\
&\le 4\pi \int_0^A \left(\frac{1}{2\varepsilon_R} p^2 + \frac{\chi_-}{2\mu} \left| f - (\frac{2}{r} p + p') \right|^2 + \frac{\chi_+}{2} \left| f - (\frac{2}{r} p + p') \right|^2 \right) r^2 dr + 4\pi g p(A) A^2 \\
&= J_{R,\mu}[p]. \qquad \text{(A.1)}
\end{aligned}
$$

The inequality $I_R[\phi] \le J_R[p]$ for any $\phi \in X$ and $p \in Y_0$ can be proved similarly.

By part (1), $p_{R,\mu} = -\varepsilon_R \phi'_{R,\mu}$ satisfies

$$
(r^2 p_{R,\mu})' = (f - \mu \phi_{R,\mu}) r^2 \quad \text{in } (0, R) \quad \text{and} \quad (r^2 p_{R,\mu})' = (f - \phi_{R,\mu}) r^2 \quad \text{in } (R, A). \qquad \text{(A.2)}
$$

These, together with the fact that $\phi_{R,\mu} \in X$, implies that $p_{R,\mu} \in Y$. Moreover, the first inequality in (A.1) becomes an equality with $\phi_{R,\mu}$ and $p_{R,\mu} = -\varepsilon_R \phi'_{R,\mu}$ replacing ϕ and p. The second inequality in (A.1) also becomes an equality by (A.2) and the definition of the Legendre transform. Thus, by the convexity of $J_{R,\mu}$, $p_{R,\mu}$ is the unique minimizer of $J_{R,\mu}$ over Y. Similarly, p_R is the unique minimizer of J_R over Y_0.

(3) By the same argument used in proving part (2) of Theorem 3.3, we have $\|\phi_{R,\mu} - \phi_R\|_\omega \to 0$ and $\max_{\phi \in X} I_{R,\mu}[\phi] \to \max_{\phi \in X} I_R[\phi]$ as $\mu \to 0$. These and part (2) imply $\|p_{R,\mu} - p_R\|_Y \to 0$ and $\min_{p \in Y} J_{R,\mu}[\phi] \to \min_{p \in Y_0} J_R[p]$ as $\mu \to 0$. □

Acknowledgment

This work was supported in part by the National Science Foundation (NSF) through the grant DMS-1913144 and DMS-2208465. The authors thank Professor Li-Tien Cheng, Dr. Benjamin Ciotti, Dr. Shuang Liu, and Dr. Zirui Zhang for helpful discussions.

References

[1] D. Andelman. Electrostatic properties of membranes: The Poisson–Boltzmann theory. In R. Lipowsky and E. Sackmann, editors, *Handbook of Biological Physics*, volume 1, pages 603–642. Elsevier, 1995.

[2] D. Bashford and D. A. Case. Generalized Born models of macromolecular solvation effects. *Ann. Rev. Phys. Chem*, 51:129–152, 2000.

[3] R. Blossey, A. C. Maggs, and R. Podgornik. Structural interactions in ionic liquids linked to higher-order Poisson–Boltzmann equations. *Phys. Rev. E*, 95:060602, 2017.

[4] J. Che, J. Dzubiella, B. Li, and J. A. McCammon. Electrostatic free energy and its variations in implicit solvent models. *J. Phys. Chem. B*, 112:3058–3069, 2008.

[5] L.-T. Cheng, B. Li, M. White, and S. Zhou. Motion of a cylindrical dielectric boundary. *SIAM J. Appl. Math.*, 73:594–616, 2013.

[6] B. Ciotti and B. Li. Legendre transforms of electrostatic free-energy functionals. *SIAM J. Applied Math.*, 78(6):2973–2995, 2018.

[7] S. Dai, B. Li, and J. Lu. Convergence of phase-field free energy and boundary force for molecular solvation. *Arch. Rational Mech. Anal.*, 227(1):105–147, 2018.

[8] M. E. Davis and J. A. McCammon. Electrostatics in biomolecular structure and dynamics. *Chem. Rev.*, 90:509–521, 1990.

[9] J. Dzubiella, J. M. J. Swanson, and J. A. McCammon. Coupling hydrophobicity, dispersion, and electrostatics in continuum solvent models. *Phys. Rev. Lett.*, 96:087802, 2006.

[10] R. Fletcher. *Practical Methods of Optimization.* John Wiley & Sons, 2nd edition, 1987.

[11] F. Fogolari and J. M. Briggs. On the variational approach to Poisson–Boltzmann free energies. *Chem. Phys. Lett.*, 281:135–139, 1997.

[12] M. K. Gilson, M. E. Davis, B. A. Luty, and J. A. McCammon. Computation of electrostatic forces on solvated molecules using the Poisson–Boltzmann equation. *J. Phys. Chem.*, 97:3591–3600, 1993.

[13] B. Li. Continuum electrostatics for ionic solutions with nonuniform ionic sizes. *Nonlinearity*, 22:811–833, 2009.

[14] B. Li. Minimization of electrostatic free energy and the Poisson–Boltzmann equation for molecular solvation with implicit solvent. *SIAM J. Math. Anal.*, 40:2536–2566, 2009.

[15] B. Li., X.-L. Cheng, and Z.-F. Zhang. Dielectric boundary force in molecular solvation with the Poisson–Boltzmann free energy: A shape derivative approach. *SIAM J. Applied Math*, 71(10):2093–2111, 2011.

[16] B. Li, P. Liu, Z. Xu, and S. Zhou. Ionic size effects: Generalized Boltzmann distributions, counterion stratification, and modified Debye length. *Nonlinearity*, 26:2899–2922, 2013.

[17] B. Li, H. Sun, and S. Zhou. Stability of a cylindrical solute-solvent interface: Effect of geometry, electrostatics, and hydrodynamics. *SIAM J. Applied Math.*, 75(3):907–928, 2015.

[18] B. Li, Z. Zhang, and S. Zhou. The calculus of boundary variations and the dielectric boundary force in the poisson–boltzmann theory for molecular solvation. *J. Nonlinear Sci.*, 31(89):1–50, 2021.

[19] D. C. Liu and J. Nocedal. On the limited memory BFGS method for large scale optimization. *Math. Program.*, 45:503–528, 1989.

[20] B. Lu, X. Cheng, J. Huang, and J. A. McCammon. Order N algorithm for computation of electrostatic interaction in biomolecular systems. *Proc. Natl. Acad. Sci. USA*, 103:19314–19319, 2006.

[21] A. C. Maggs. A minimizing principle for the Poisson–Boltzmann equation. *Europhys. Lett.*, 98:16012, 2012.

[22] A. C. Maggs and R. Podgornik. General theory of asymmetric steric interactions in electrostatic double layers. *Soft Matter*, 12:1219–1229, 2016.

[23] J. S. Pujos and A. C. Maggs. Convexity and stiffness in energy functions for electrostatic simulations. *J. Chem. Theory Comput.*, 11:1419–1427, 2015.

[24] R. Pytlak. *Conjugate Gradient Algorithms in Nonconvex Optimization.* Springer, 2008.

[25] E. S. Reiner and C. J. Radke. Variational approach to the electrostatic free energy in charged colloidal suspensions: General theory for open systems. *J. Chem. Soc. Faraday Trans.*, 86:3901–3912, 1990.

[26] R. T. Rockafellar. *Convex Analysis*. Princeton University Press, 1970.

[27] K. A. Sharp and B. Honig. Calculating total electrostatic energies with the nonlinear Poisson–Boltzmann equation. *J. Phys. Chem.*, 94:7684–7692, 1990.

[28] K. A. Sharp and B. Honig. Electrostatic interactions in macromolecules: Theory and applications. *Annu. Rev. Biophys. Biophys. Chem.*, 19:301–332, 1990.

[29] H. Sun, J. Wen, Y. Zhao, B. Li, and J. A. McCammon. A self-consistent phase-field approach to implicit solvation of charged molecules with Poisson–Boltzmann electrostatics. *J. Chem. Phys.*, 143:243110, 2015.

[30] R. Temam. *Navier–Stokes Equations: Theory and Numerical Analysis*. North-Holland, 3rd edition, 1984.

[31] Z. Wang, J. Che, L.-T. Cheng, J. Dzubiella, B. Li, and J. A. McCammon. Level-set variational implicit solvation with the Coulomb-field approximation. *J. Chem. Theory Comput.*, 8:386–397, 2012.

[32] S. Zhou, L.-T. Cheng, J. Dzubiella, B. Li, and J. A. McCammon. Variational implicit solvation with Poisson–Boltzmann theory. *J. Chem. Theory Comput.*, 10:1454–1467, 2014.

[33] S. Zhou, Z. Wang, and B. Li. Mean-field description of ionic size effects with non-uniform ionic sizes: A numerical approach. *Phys. Rev. E*, 84:021901, 2011.

[34] R. K. P. Zia, E. F. Redish, and S. R. McKay. Making sense of the Legendre transform. *Amer. J. Phys.*, 77:614–622, 2009.